IMPROVING WATER REFLECTANCE RETRIEVAL FROM MODIS IMAGERY IN THE HIGHLY TURBID WATERS OF LA PLATA RIVER

A. I. Dogliotti[1,2], K. Ruddick[1], B. Nechad[1], and C. Lasta[3]

[1] Royal Belgian Institute of Natural Sciences, Management Unit of the North Sea Mathematical Models (RBINS/MUMM), Belgium;
[2] Instituto de Astronomía y Física del Espacio (IAFE), CONICET-UBA, Argentina. ana.dogliotti@mumm.ac.be
[3] Instituto Nacional de Investigación y Desarrollo Pesquero (INIDEP), Mar del Plata, Argentina.

ABSTRACT

The accurate retrieval of marine reflectance from remotely sensed data depends on the effective removal of the contribution of the atmosphere to the total signal that reaches the sensor at the top of the atmosphere, i.e. the atmospheric correction process. This is particularly important in highly turbid waters where assumptions made by traditional atmospheric correction algorithms for open ocean waters are often invalid. We have analyzed three different atmospheric correction algorithms in the challenging turbid waters of La Plata River estuary located in the western Atlantic coast at ~35° S. Three algorithms were applied to Moderate Resolution Imaging Spectroradiometer (MODIS) images of the region, the standard near-infrared (NIR) algorithm and two algorithms that use the short wave infrared (SWIR) bands. The two SWIR algorithms differ in the way the aerosol model is selected. The standard NIR atmospheric correction completely failed in retrieving water reflectance in the river plume waters mainly due to sensor saturation and an incorrect estimation of the marine contribution in the NIR. The standard SWIR approach showed better results, but unphysical correlations between marine features and atmospheric products, such as aerosol reflectance, in the most turbid part of the estuary were clearly identified. The use of an iterative SWIR-based atmospheric correction approach that accounts for non-zero water reflectance in the SWIR bands seems to be a good alternative for retrieving accurate marine reflectance. The difference in the derived water reflectance between the two SWIR approaches showed a spectral dependence, being higher in the shorter wavelengths and lower in the NIR. A comparison between MODIS-derived turbidity values from the different atmospheric correction approaches and *in situ* data showed no significant differences mainly because the one-band turbidity algorithm applied uses the 859 nm band where differences between the approaches are lower.

1. INTRODUCTION

Satellite ocean color sensors, like the Moderate Resolution Imaging Spectroradiometer onboard the Aqua platform (MODIS-Aqua), have demonstrated to be useful for retrieval of in-water constituent concentrations, especially in the open ocean. However, their use in coastal and particularly in turbid waters has been hindered by difficulties with atmospheric correction. The standard atmospheric correction algorithm developed by the National Aeronautics and Space Administration (NASA) Ocean Biology Processing Group relies on the assumption of negligible water-leaving reflectance in the near-infrared (NIR) region of the spectrum (black pixel assumption) for the open ocean with modifications to account for the water-leaving reflectance contribution in the NIR bands for more coastal moderately turbid waters (Stumpf *et al.* 2003, Bailey *et al.* 2010). Alternatively, an atmospheric correction has been developed that uses the short wave infrared (SWIR) bands and assumes negligible water-leaving radiance due to the high water absorption in this part of the spectrum (Wang 2007). This algorithm has shown to perform well in retrieving derived products in turbid coastal waters (Wang & Shi, 2005, Wang 2007, Wang *et al.* 2007, 2009a). Also a combined NIR-SWIR atmospheric correction approach has been proposed which make use of a turbidity index (T_{ind}, Shi & Wang 2007) calculated on a pixel-by-pixel basis to determine which atmospheric correction method to use. The NIR-based method is used in the non-turbid waters, while the SWIR approach is used in turbid waters where the turbidity index exceeds a certain threshold. Improved ocean color products have been retrieved using this combined approach (Wang *et al.* 2009b). However, Werdell *et al.* (2010) found that in the Chesapeake Bay the use of the SWIR approach produced broad and flat frequency distributions of normalized water-leaving radiance (*nLw*) compared to the ones obtained using the NIR approach mainly due to the low signal-to-noise ratios (SNR) of the SWIR bands. Nevertheless, they found an improvement in chlorophyll concentration retrieval using the combined NIR-SWIR method in this region, but at the cost of increased number of pixels of negative normalized water-leaving radiance and decreased sample size.

Moreover, in extremely turbid waters, such as the Hangzhou Bay in China, it has been found that the SWIR 1240 nm band is not always black (Shi & Wang 2009a).

La Plata River estuary, located in the western Atlantic coast at ~35° S, is a shallow (<10 m) and large-scale estuary (Figure 1) which drains the second largest basin in South America and is considered among the most turbid rivers in the world with mean values of total suspended matter (TSM) concentration ranging from 100 to 300 mg L^{-1} (Urien, 1967; C.A.R.P., 1989). A surface turbidity front generally associated to the turbidity maximum is a persistent structure that is a characteristic feature of the estuary (Framiñan 2005). It's mean position have been found to be strongly related to the bottom topography (Framiñan & Brown 1996) following a shallow bar at the mouth of the river that runs between Punta Piedras and Montevideo (Figure 1).These extremely turbid waters represent a challenge and an ideal scenario to test atmospheric correction algorithm performance (Shi & Wang 2009, Doerffer 2006, Moore *et al*. 2010, Doron *et al*. 2011).

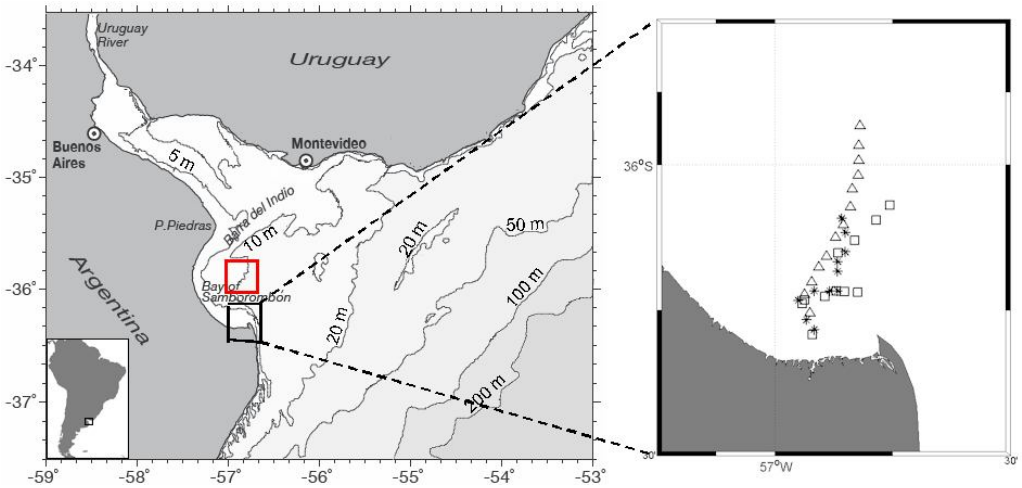

Figure 1. Maps of La Plata River estuary with indication of the locations of the sampled stations during three campaigns carried on Dec 20, 2010 (□), Mar 21, 2011 (✳) and Apr 27, 2011 (△). The red polygon bounds the clear water pixels region used to retrieve the aerosol model (see further in the text).

The objective of the present work is to retrieve better estimates of water reflectance in the highly turbid waters of La Plata River estuary to further retrieve in-water constituent concentration, such as turbidity and/or total suspended matter concentration. Therefore, we analyze the NIR and NIR-SWIR atmospheric correction approaches as well as an iterative SWIR-based atmospheric correction algorithm, as proposed by Wang *et al*. (2011), to account for non-zero water reflectance in the SWIR bands over the extremely turbid waters found in this region. Then, turbidity is computed from the reflectance values obtained from the different atmospheric correction approaches using a one-band algorithm (Nechad *et al.* 2009) and is compared to *in situ* measurements.

2. METHODS

2.1. Data and Methods

MODIS-Aqua spatially extracted Level-1A files were acquired for La Plata River estuary (Figure 1) from the NASA ocean color web page (oceancolor.gsfc.nasa.gov) for the dates with concurrent *in situ* turbidity measurements. The SeaDAS 6.2 (update 2a) software was used to generate Level-2 files containing spectral Rayleigh-corrected (ρ_{rc}) reflectance, the turbidity index (T_{ind}), aerosol radiance (L_a), and remote sensing reflectance (R_{rs}). Aerosol reflectance (ρ_a) was calculated following Gordon & Wang (1994) definition: $\rho = \pi L / F_0 \cos\theta_0$, where L is the radiance in a given solar and viewing geometry, F_0 is the extraterrestrial solar irradiance and θ_0 is the solar zenith angle. Water reflectance (ρ_w) was calculated from the remote sensing reflectance (R_{rs}) as $\rho_w = R_{rs}\,\pi$.

Three different atmospheric correction approaches were applied to L1A data (see flow chart in Figure 2):

1) The standard NIR atmospheric approach, which uses the 748 and 869 nm bands and corrections to account for NIR ocean contribution estimated from the 667 nm band.

2) The NIR-SWIR switching algorithm, which was applied using the 1240 and 2130 nm bands when T_{ind}>1.3 as in Shi & Wang (2007), and
3) An iterative approach of the SWIR atmospheric correction algorithm is used for the turbid waters, i.e. when T_{ind}>1.3, as proposed and implemented in Wang *et al.* (2011).

The third approach requires running the atmospheric correction twice; first the 1240 and 2130 nm SWIR bands are used to retrieve the aerosol model (Ångström exponent) on a pixel-by pixel basis. Ångström exponent at 531 nm, α(531), from a region of clear water pixels is used to determine the aerosol model since each model has a unique value of α(531) (Wang, 2007). The mean value of α(531) from a region of relatively clear waters (30x30 pixels) located in the center of Samborombón bay (red polygon in Figure 1) is extracted from each scene. Then, a second run of the atmospheric correction is applied to the turbid waters using a fixed α(531) obtained from the clear water pixels and information on aerosol concentration is taken from 2130 nm band. This approach assumes a fixed aerosol model for the whole image and will be referred hereafter as SWIR-F, while the standard SWIR approach which uses a variable aerosol model estimated in a pixel-by-pixel basis will be referred as SWIR-V.

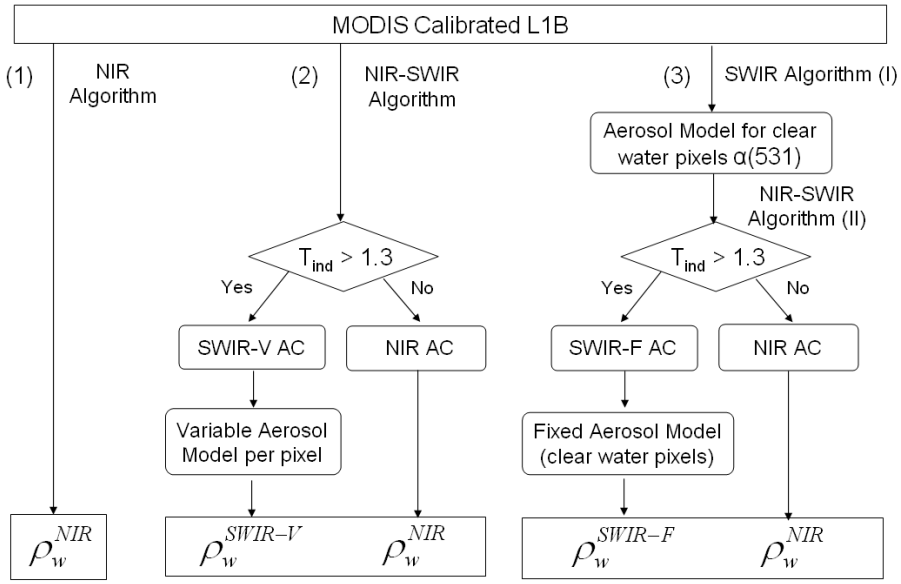

Figure 2. Flow chart of the different atmospheric correction (AC) approaches applied to MODIS-Aqua imagery and analyzed in the present study.

The cloud-masking was performed using the Rayleigh-corrected reflectance (dimensionless) at 2130 nm and a threshold of 0.018. This filters out only clouds, while the operational scheme usually erroneously masks the highly turbid waters as clouds.

Turbidity measurements were performed on surface samples obtained in three cruises on board Guardacostas 122 "LAGO MASCARDI" vessel in Dec 20, 2010, Mar 21, and Apr 27, 2011 (Figure 1), using the Multi Parameter Water Quality Monitoring System HORIBA, model U-22XD. Further details on the methodology used can be found in Dogliotti *et al.* (2011).

For the comparison between satellite-derived turbidity and *in situ* measurements ("match-up"), satellite-derived water reflectance values of a 3x3 pixel box centred at the location of the sample sites were extracted and statistics were calculated. If the coefficient of variation was < 0.2, the median value of all unmasked pixels was used as input to test the one-band turbidity algorithm (Nechad *et al.* 2009). The time difference between the field measurements and the satellite overpass varied between 5 minutes to 4 hours.

3. RESULTS AND DICUSSION

3.1 Water reflectance from NIR, SWIR-V and SWIR-F approaches

The application of the standard NASA (NIR) atmospheric correction systematically failed to retrieve water reflectance from the highly turbid waters of La Plata River estuary. The main reason is saturation of MODIS ocean bands. The retrieval of water reflectance is not possible due to saturation of the MODIS 667, 748 and

869 nm bands which are used in the NIR atmospheric correction (Stumpf *et al.* 2003, Bailey *et al.* 2010). As a result the whole estuary is generally masked in the ocean bands, while negative values are retrieved in the high resolution (250 and 500 m) land bands mimicking the high turbid water plume (Figure 3). Only results obtained from the processing of the MODIS-Aqua image acquired on Dec 10, 2010 will be shown in the following sections, but similar results were obtained for the other processed imaged.

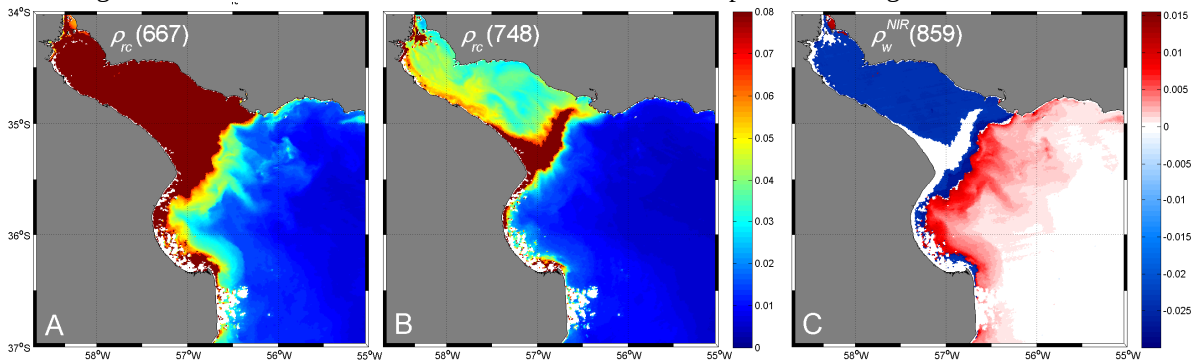

Figure 3. MODIS-Aqua Rayleigh-corrected reflectance at A) 667, B) 748 nm bands, and C) water reflectance at 859 nm band obtained using the standard NIR AC approach on Dec 20, 2010 over La Plata estuary region. Band saturation and clouds are shown in brown and white, respectively.

The turbidity index (T_{ind}) proposed by Shi & Wang (2007), which uses the 748, 1240 and 2130 nm bands and that is used to switch between the NIR and SWIR atmospheric correction approaches, was calculated (Figure 4). Most of the pixels in the study region had T_{ind} values higher than 1.3 (threshold recommended by Shi & Wang 2007), thus most of the study region is considered as turbid waters and the SWIR approach is used.

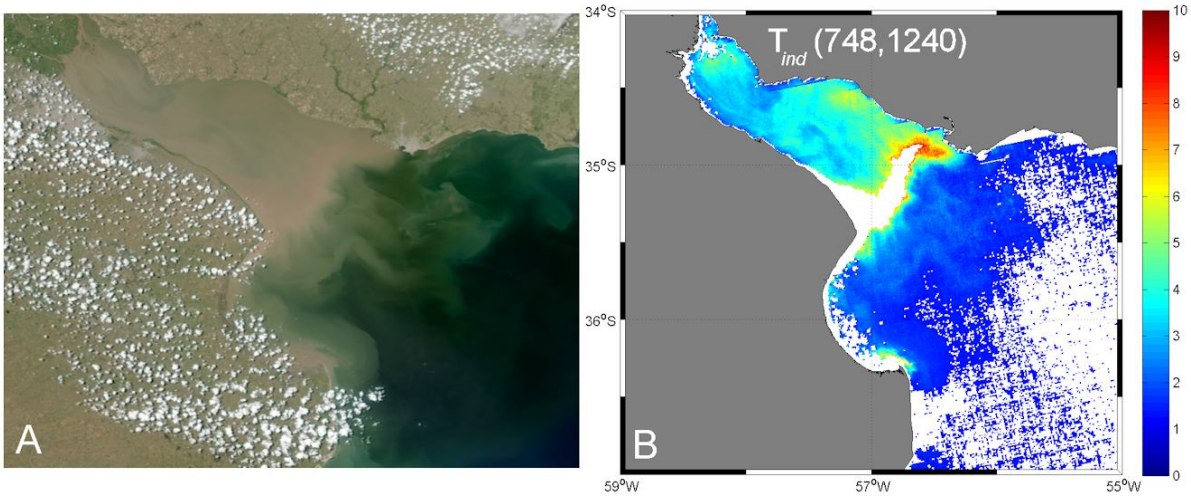

Figure 4. A) MODIS-Aqua true color image and B) Turbidity index for La Plata Estuary region on Dec 20, 2010. Masked pixels due to clouds, 748nm band saturation, or T_{ind}<1.3 are shown in white.

The two different SWIR atmospheric correction approaches, the SWIR-V and SWIR-F, will be evaluated for turbid pixels only, i.e. those with T_{ind}>1.3. The SWIR-F approach retrieved a lower frequency of negative ρ_w. The percentage of negative ρ_w decreased from 1.022 to 0.004, from 0.617 to 0.004, and from 0.043 to 0% at 412, 443 and 448 nm, respectively, for the MODIS-Aqua image on Dec 20, 2010.

Figure 5 shows the MODIS-Aqua retrieved Rayleigh-corrected (top of atmosphere), aerosol and water reflectance at 412 nm on Dec 20, 2010 using the SWIR-V approach. Relatively high ρ_a^{SWIR-V} values can be observed where the maximum turbidity front is known to occur (Barra del Indio shoal) and which is correlated to relative lower ρ_w^{SWIR-V}. This unphysical correlation between the atmospheric ρ_a(412) product and a marine feature is a consequence of the non negligible water reflectance in the 1240 nm SWIR band in the most turbid region, as was previously found in Shi & Wang (2009). Invalidity of the SWIR black pixel assumption leads to an overestimation of ρ_a^{SWIR-V} and consequently to an underestimation of ρ_w^{SWIR-V}, with greatest underestimation in the blue bands.

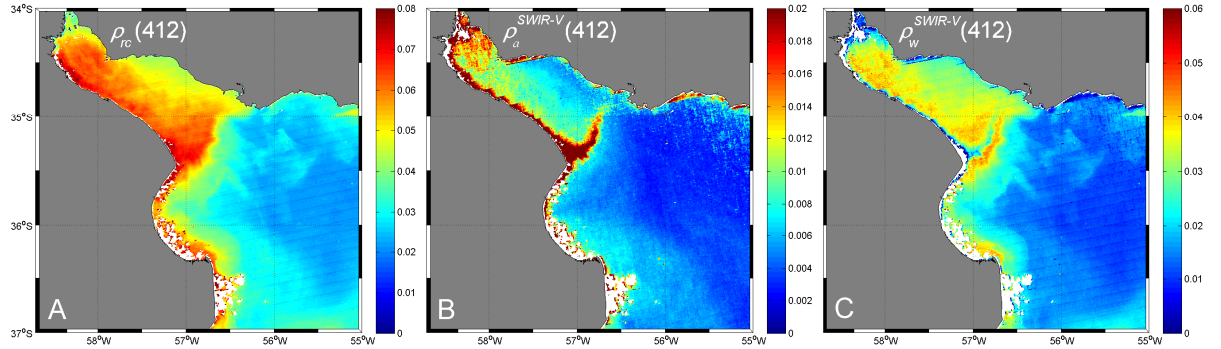

Figure 5. A) Rayleigh-corrected reflectance, B) aerosol and C) water reflectance at 412 nm retrieved from MODIS-Aqua image on Dec. 20, 2010 using the SWIR-V approach.

On the other hand, when the SWIR-F atmospheric correction approach is applied, the spatial distribution of $\rho_a^{SWIR-F}(412)$ and $\rho_w^{SWIR-F}(412)$ show no correlation with the highly turbid front (Figure 6) indicating a more realistic separation of top-of-atmosphere radiance into atmospheric and marine components.

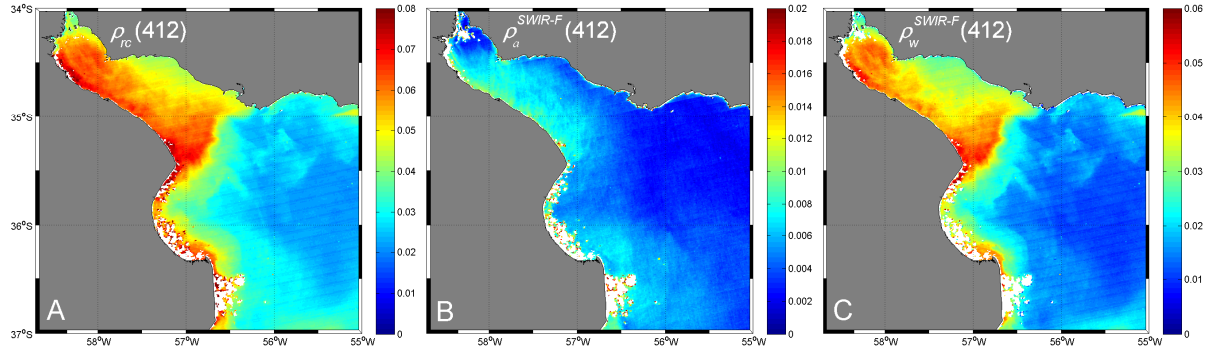

Figure 6. A) Rayleigh-corrected reflectance, B) aerosol and C) water reflectance at 412 nm retrieved from MODIS-Aqua image on Dec 20, 2010 using the SWIR-F approach.

The differences in the retrieved ρ_w when comparing the SWIR-V and SWIR-F approaches are compared to determine their spectral dependence and relation to turbidity (if any). The mean and standard deviation of the ratio between ρ_w^{SWIR-F} and ρ_w^{SWIR-V} were obtained from a 5x5 window at different locations within the La Plata River estuary (Figure 7 and Table 1).

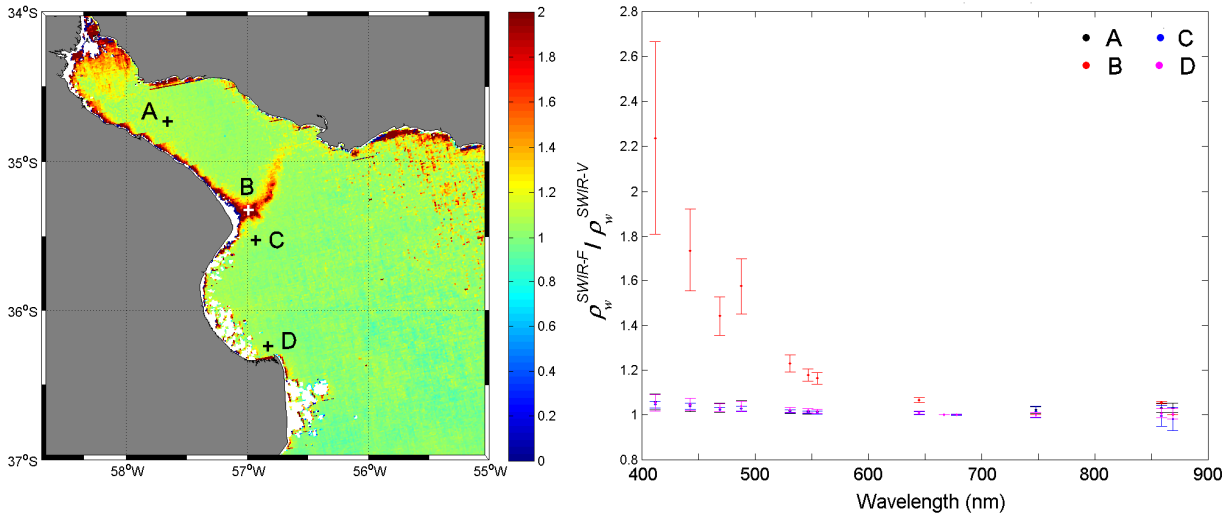

Figure 7. Ratio between ρ_w^{SWIR-F} and ρ_w^{SWIR-V} at 412 nm calculated from MODIS-Aqua image on Dec 20, 2010; Map (left) and mean and standard deviation at all bands from the locations indicated in the map (right).

The highest ratios were found at the blue bands (~400 nm) and where the most turbid waters are known to occur. Figure 7 shows that at the turbidity front (location indicated as B) where the maximum turbidity is known to occur, the mean ratio decreases from 2.2 at 412 nm to 0.4 at 869 nm. At the upper (location A) and in the southern Samborombón bay (location D) locations, with relatively high turbidity, the mean ratios varied less (between 1.058 and 1.055 at 412 nm to 1.031 and 1.004 at 869 nm, respectively). At the location situated in the more clear waters (east of the turbidity front) the mean ratios were relative lower varying from 1.045 at 412 nm to 0.982 at 869 nm (location C). Missing values in Table 1 at 667, 678 and 748 nm are due to band saturation.

Table 1. Mean ratio of ρ_w^{SWIR-F} to ρ_w^{SWIR-V} and standard deviation from MODIS-Aqua bands on Dec 20, 2010 at the locations indicated in Figure 7.

	412	*443*	*469*	*488*	*531*	*547*	*555*	*645*	*667*	*678*	*748*	*859*	*869*
A	1.06 (±0.04)	1.05 (±0.03)	1.04 (±0.03)	1.03 (±0.02)	1.02 (±0.01)	1.02 (±0.01)	1.01 (±0.01)	1.01 (±0.01)	-	-	1.02 (±0.01)	1.03 (±0.02)	1.03 (±0.02)
B	2.24 (±0.43)	1.74 (0.18)	1.58 (0.13)	1.44 (0.09)	1.23 (0.04)	1.18 (0.03)	1.16 (0.03)	1.07 (0.01)	-	-	-	1.05 (0.01)	-
C	1.05 (±0.02)	1.04 (0.01)	1.03 (0.01)	1.02 (0.01)	1.01 (0.01)	1.01 (0.01)	1.01 (0.01)	1.01 (0.01)	-	-	1.01 (0.03)	0.99 (0.05)	0.98 (0.05)
D	1.06 (0.04)	1.05 (0.03)	1.04 (0.02)	1.03 (0.02)	1.02 (0.01)	1.02 (0.01)	1.02 (0.01)	1.01 (0.01)	-	-	-	1.01 (0.02)	1.00 (0.02)

3.2. Turbidity from SWIR-V and SWIR-F approaches

Turbidity was calculated using the one-band turbidity algorithm (Nechad *et al.* 2009) applied to satellite-derived water reflectance at the 859 nm band and compared to *in situ* measurements. Figure 8 shows results of the turbidity match-up corresponding to MODIS-Aqua data processed using the SWIR-V and SWIR-F approaches.

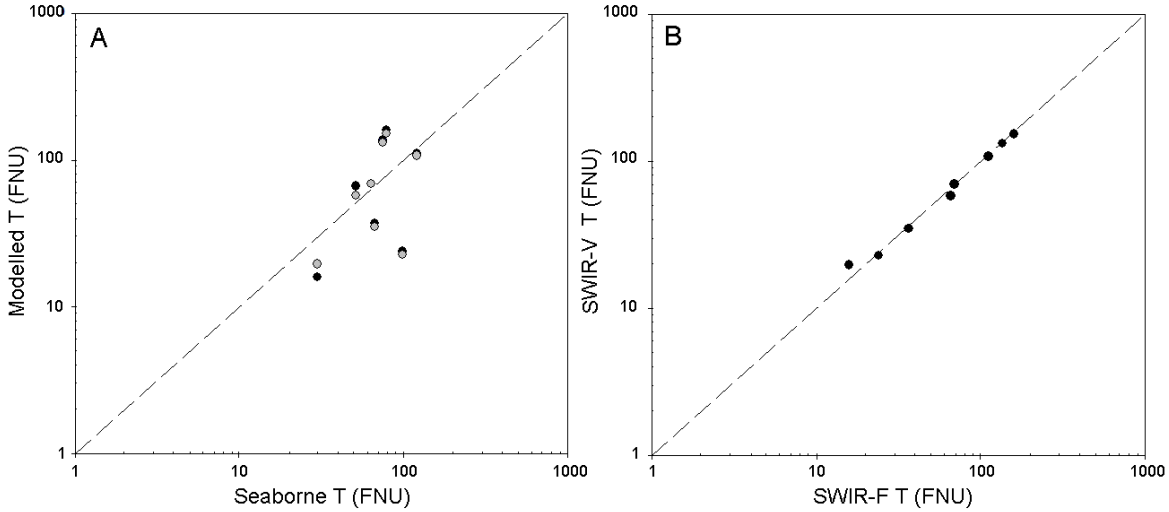

Figure 8. A) Scatter plot of seaborne and modelled turbidity (T) using the SWIR-V (grey) and SWIR-F (black) atmospheric correction approaches for stations with T_{ind}>1.3; B) Comparison of MODIS-derived T from the two approaches.

Table 2 summarizes the match-up values of the slope, intercept, correlation coefficient (*R*), absolute percentage difference (*APD*), mean ratio, and the root-mean-square of the $\log_{10}$-dfference error between MODIS-derived and *in situ* measured values. The number of data was the same for the two approaches (*N*= 8). In general, similar statistics were obtained when comparing the satellite-derived values using both methods, with relatively low correlation (~0.5) and mean ratio close to 1. The SWIR-F method showed slope closer to 1, lower $\log_{10}$-RMS, but higher mean percent difference.

Table 2. Turbidity match-up statistics for MODIS-Aqua data processed using the SWIR-F and SWIR-V atmospheric correction approaches.

Algorithm	*Slope*	*Intercept*	*R*	*APD(%)*	*Ratio*	*Log_{10}RMS*	*N*
T_{859}(SWIR-F)	1.02	- 0.1005	0.52	49.6	1.06	0.3852	8
T_{859}(SWIR-V)	0.88	0.1553	0.47	45.3	1.03	0.4196	8

In order to analyze the overall relative difference in the estimation of turbidity for the two SWIR approaches, the relative percentage difference between the MODIS-derived turbidity using the two different approaches was calculated using all the "turbid" pixels (T_{ind}>1.3) from MODIS-Aqua image on Dec 20, 2010 (Figure 9). In general, the relative difference was low, varying in ±2%. The slightly non-zero slope apparent for the high turbidity data of Figure 9 arises from the non-zero 1240nm water reflectance in the SWIR-F algorithm.

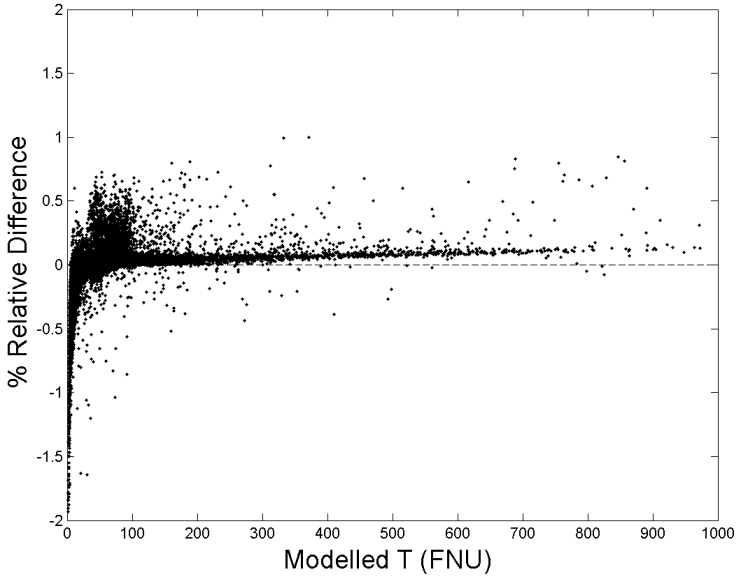

Figure 9. Relative percentage difference of the satellite-derived turbidity form MODIS-Aqua image of Dec 20, 2010 processed using SWIR-V and SWIR-F atmospheric approaches. Only pixels with T_{ind}>1.3 are considered.

4. CONCLUSIONS

In the present study different atmospheric correction algorithms were tested in the turbid waters of La Plata River estuary. We showed that the standard NIR atmospheric correction completely fails in retrieving water reflectance mainly due to sensor saturation and hence an incorrect estimation of the marine contribution in the NIR. The standard SWIR approach (which calculates the aerosol model in a pixel-by-pixel basis) clearly showed better results, but still some over-estimation of aerosol reflectance in the most turbid part of the estuary, leading to an underestimation of water reflectance (retrieving negative values in the blue bands). This indicates that the black pixel assumption in the 1240 nm SWIR band also fails in these extremely turbid waters as was previously suggested by Shi & Wang (2009). The use of a spatially constant aerosol model determined from clear waters proved to be a good alternative for the processing of MODIS-Aqua in the most turbid region of the estuary. Using a fixed aerosol model, the frequency of negative pixels in the blue bands was greatly reduced and the spatial distribution of the atmospheric products, such as aerosol reflectance, showed no unrealistic correlation with marine (bathymetric) features. The differences found between the retrieved ρ_w using the two different SWIR approached showed a spectral dependence, higher in the blue bands, and related to the amount of suspended particulate matter, with higher differences found in the most turbid regions. However, no significant differences were found between the two approaches in the derived turbidity values. This is mainly due to the fact that the differences in ρ_w from the two approaches are low in the NIR bands, including the 859 nm band which is used to retrieve turbidity. Therefore, the modification of the SWIR atmospheric correction used seems to improve the retrieval of water reflectance in these highly turbid waters. In a next step *in situ* reflectance measurements will be used to validate more directly the satellite-derive estimates.

ACKNOWLEDGEMENTS

This study was funded by the Belgian Science Policy Office (BELSPO) in the framework of a post-doctoral visit (BELCOLOUR-ARG project), and of the STEREO/BELCOLOUR-2 Project, and by CONICET. The MODIS-Aqua Level 1A data were obtained from NASA/GES DAAC. The Gral. Lavalle Detachment PNA and the staff of the vessel "GC 122" are thanked for their help with the seaborne measurements in Samborombón Bay.

REFERENCES

Bailey, S. W., Franz, B. A., & Werdell, P. J. (2010). Updated NIR water-leaving radiance estimation for ocean color data processing. *Optics Express*, 18, 7521−7527.

CARP, 1989. Estudio para la evaluacion de la contaminación en el Río de la Plata. Capítulo I. Aspectos Geológicos. Comisión Administradora del Río de la Plata, Buenos Aires, pp. 1–72.

Doerffer, R. (2006). MERIS Case 1 Validation: Performance of the NN case 2 water algorithm for case 1 water. *MERIS Validation Team Meeting*, ESA ESRIN, Frascati, Italy.

Dogliotti, A. I., Ruddick, K., Nechad, B., Lasta, C., Mercado, A. Hozbor, C., Guerrero, R. Riviello Lopez, G. & Abelando, M. (2011). Mapping turbidity using ocean color data over La Plata River Estuary, Argentina. *Proceeding of 5th EARSeL Workshop on Remote Sensing of the Coastal Zone*, Prague, Czech Republic.

Doron, M, Bélanger, S., Doxaran, D. & Babin, M. (2011). Spectral variations in the near-infrared ocean reflectance. *Remote Sensing of Environment*, 15, 1617-1631.

Framiñan, M., & O. Brown (1996), Study of the Río de la Plata turbidity front, Part 1: Spatial and temporal distribution, *Cont. Shelf Res.*, 16, 1259– 1282, doi:10.1016/0278-4343(95)00071-2.

Framiñan, M. (2005). On the physics, circulation and exchange processes of the Río de la Plata estuary and the adjacent shelf, Ph.D. dissertation, 486 pp., Rosenstiel Sch. of Mar. and Atmos. Sci., Univ. of Miami, Fla.

Gordon, H. R., & Wang, M. (1994). Retrieval of water-leaving radiance and aerosol optical thickness over the oceans with SeaWiFS: A preliminary algorithm. *Applied Optics*, 33, 443−452.

Moore, G., Lavender, S., Kratzer, S., Icely, J. & Huot, J-P. (2010). The MERIS bright pixel atmospheric correction: evolution, performance assessment and validation for the MERIS 3rd reprocessing. *Proceedings of the Ocean Optics XX Conference* held in Anchorage, USA.

Nechad, B., Ruddick, K. G., & Neukermans, G. (2009). Calibration and validation of a generic multisensor algorithm for mapping of turbidity in coastal waters. In: *SPIE, Remote Sensing of the Ocean, Sea Ice, and Large Water Regions*, Berlin, Germany. Vol. 7473, 74730H.

Stumpf, R. P., Arnone, R. A., Gould, R. W., Jr., Martinolich, P. M., & Ransibrahmanakul, V. (2003). A partially coupled ocean-atmosphere model for retrieval of water-leaving radiance from seawifs in coastal waters. NASA Tech. Memo. 206892, National Aeronautics and Space Administration, Goddard Space Flight Center, Greenbelt, MD.

Shi, W., & Wang, M. (2007). Detection of turbid waters and absorbing aerosols for the MODIS ocean color data processing. *Remote Sensing of Environment*, 110, 149−161.

Shi, W., & Wang, M. (2009). An assessment of the black ocean pixel assumption for MODIS SWIR bands. *Remote Sensing of Environment*, 113, 1587−1597.

Urien, C.M. (1967). Los sedimentos modernos del Río de La Plata Exterior. *Pub. H-106, Serv. de Hidrog. Naval*, 4(2), 113-213.

Wang, M. (2007). Remote sensing of the ocean contributions from ultraviolet to nearinfrared using the shortwave infrared bands: simulations. *Applied Optics*, 46, 1535−1547.

Wang, M., & Shi, W. (2005). Estimation of ocean contribution at the MODIS nearinfrared wavelengths along the east coast of the U.S.: Two case studies. *Geophysical Research Letters*, 32, L13606. doi:10.1029/ 2005GL022917.

Wang, M., Tang, J., & Shi, W. (2007). MODIS-derived ocean color products along the China east coastal region. *Geophysical Research Letters*, 34, L06611. doi:10.1029/2006GL028599.

Wang, M., Son, S., & Harding, L.W. J. (2009a). Retrieval of diffuse attenuation coefficient in the Chesapeake Bay and turbid ocean regions for satellite ocean color applications. *Journal of Geophysical Research*, 114, C10011. doi:10.1029/2009JC005286.

Wang, M., Son, S., & Shi, W. (2009b). Evaluation of MODIS SWIR and NIR-SWIR atmospheric correction algorithm using SeaBASS data. *Remote Sensing of Environment*, 113, 635−644.

Wang, M., Shi, W, & Tang, J. (2011). Water property monitoring and assessment for China's inland Lake Taihu from MODIS-Aqua measurements. *Remote Sensing of Environment*, 115, 841−854.

Werdell, P. J., Franz, B. A., & Bailey, S. W. (2010). Evaluation of shortwave infrared atmospheric correction for ocean color remote sensing of Chesapeake Bay. *Remote Sensing of Environment*, 114, 2238−2247.